Adiabatic frictional pressure gradient during flow boiling of pure refrigerant R1233zd and non-azeotropic mixtures R448A, R452A and R455A

Adiabatic frictional pressure gradient during flow boiling of pure refrigerant R1233zd and non-azeotropic mixtures R448A, R452A and R455A

A Arcasi[1], R Mastrullo[1], A W Mauro[1*] and L Viscito[1]

[1] Department of Industrial Engineering, Federico II University of Naples, P.le Tecchio 80, 80125 Naples (Italy)
*Corresponding author e-mail: wmauro@unina.it

Abstract. The research on two-phase flow characteristics of refrigerants is of primary importance in several fields, such as air conditioning and refrigeration systems. Therefore, the determination of the pressure drop during flow boiling is important for the correct design of evaporators and heat spreaders systems. This paper presents a collection of experiments on flow boiling pressure drop using pure refrigerant R1233zd and new low-GWP refrigerant mixtures R448A, R452A and R455A. All tests were performed in adiabatic conditions, in a smooth horizontal stainless-steel tube having an internal diameter of 6.0 mm and a thickness of 1.0 mm. The effect of operating parameters, such as (bubble) saturation temperature (from 25 to 65 °C) and mass flux (from 150 to 600 kg/m^{2}s) is investigated and discussed, and the performance of the chosen fluids is also compared. Finally, an assessment of existing prediction methods is carried-out to find the most suitable correlations for two-phase pressure drop evaluation.

Keywords: *Flow boiling, low-GWP refrigerants, pressure drop, assessment*

1. Introduction

Nowadays, due to anthropic activities, the global warming issue is widely discussed. Particularly, since the early 2000s, the use of chlorofluorocarbon and hydro-chlorofluorocarbon refrigerants (CFCs and HCFCs) has been banned in several fields, with hydrofluorocarbon ones (HFCs) now being used thanks to their zero-ozone depletion potential (ODP). Nevertheless, HFC refrigerants are planned to be replaced due to their strong greenhouse effect. On this regard, the European F-Gas Regulation [1] restricts the global warming potential (GWP) value of the employed refrigerants in several sectors. For the abovementioned reasons, in the refrigerated transport sector as well as in the commercial refrigeration systems at low/medium temperature level the R404A refrigerant (GWP 3922) will be replaced with new low-GWP mixtures such as R448A (GWP 1390), R452A (GWP 2141) and R455A (GWP 148) having similar reduced pressure values. On the other hand, for low-pressure centrifugal chillers and for high temperature level systems such as organic Rankine cycles (ORC) – up to 120 °C - pure refrigerant R1233zd can be used thanks to its low reduced pressure, non-toxicity, non-flammability and GWP value equal to 1. In this context, a correct evaluation of the frictional pressure drop is useful both for a proper matching of the temperature level of the refrigerant and the secondary fluid in the evaporator and for a correct design of the system piping.

After a bibliographic research, for the abovementioned refrigerants there is a lack of frictional pressure gradient data in open literature. Some experimental studies provide two-phase pressure drop

data of pure refrigerant R1233zd [2, 3, 4] during evaporation and condensation processes, whereas Jacob et al. [5] propose a comparison between the condensation pressure drop data of R404A and the substitutes R448A and R452A mixtures. Finally, Mauro et al. [6] provide frictional pressure drop data for the R455A mixture for different saturation temperatures and mass velocities. However, we found no assessment of the existing prediction methods for all the mentioned fluids and a thorough experimental campaign for pressure drop data of these new refrigerants has not been carried-out yet. For these reasons, this paper presents frictional pressure drop data of R1233zd, R448A, R452A and R455A refrigerants. The effect of the operating parameters in terms of bubble saturation temperature (from 25 to 65 °C, close to the working conditions of heat pumps for sanitary hot water production and to ORC systems, and corresponding to reduced pressures from 0.03 to 0.81) and mass flux (from 150 to 600 kg/m^{2}s) is discussed. The performance of the employed fluids in the same operating conditions is then compared. Finally, an assessment of the prediction methods is carried-out to find, among those implemented, the most appropriate correlation for the frictional pressure gradient.

2. Experimental apparatus

2.1. Refrigerant loop, test section and measurement instrumentation

The experimental apparatus is represented in Figure 1. In the primary loop (black line) the working fluid is pumped by a gear pump into a Coriolis mass flow meter. Then, the refrigerant passes through an electric pre-heater section where it partially evaporates and the desired vapor quality value is achieved. Successively, it passes through the test section where the pressure drop is measured; finally, the saturated fluid condenses into a plate heat exchanger and goes into a liquid receiver and a sub-cooler before closing the loop with the pump suction head. More information about the whole experimental test rig and its components can be found in previous publications of the same authors [7,8].

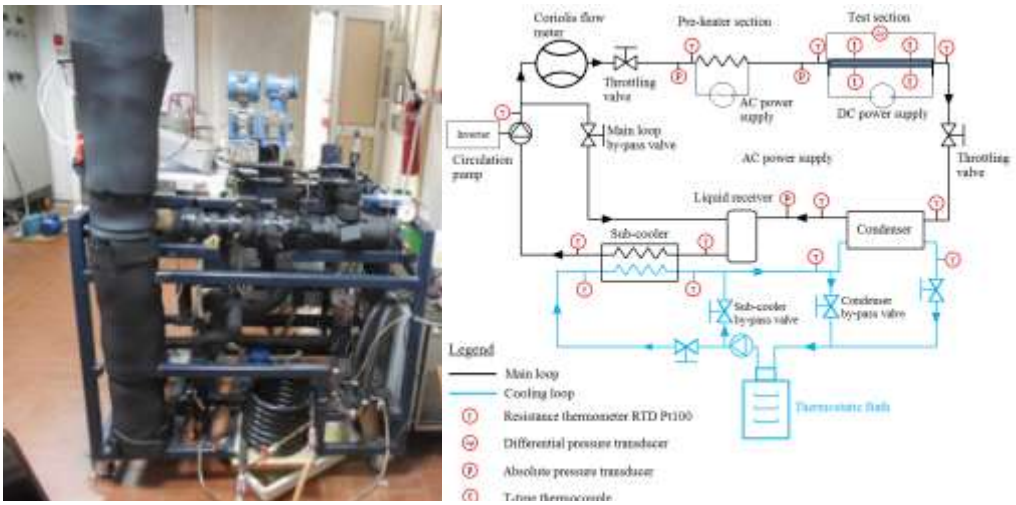

Figure 1. Photograph of the experimental apparatus and its schematic representation.

Table 1. Summary of operative range and accuracy of the measurement instrumentation.

Measurement	Range	Instrumental accuracy
Temperature	-80/250 °C	± 0.180 °C
Inlet absolute pressure (test section)	0/35 bar	± 0.1% reading
Absolute pressure (test rig)	0/50 bar	± 0.3% reading
Differential pressure (test section)	0/14.51 kPa	± 0.06 kPa
Flow meter	2.3/115.7 g/s	± 1.0% reading
Electric power	0/3.6 kW	± 1.0% reading

The test section is made of a horizontal stainless-steel tube (AISI SS316) having an inner diameter of 6.00 ± 0.05 mm and an external diameter of 8.0 ± 0.05 mm. Two pressure taps at a distance of 237 ± 0.91 mm are used both for the evaluation of the pressure drop across the test tube and the inlet absolute pressure value. Table 1 provides a summary of the instrument specifications of transducers and sensors employed for this experimental campaign.

3. Method

3.1. Data reduction and uncertainty analysis

The frictional pressure gradient across the test section is directly obtained by the pressure drop measurement. In fact, the gravitational contribution has not been considered due to the horizontal test section layout and the momentum contribution can be neglected since all tests are performed in adiabatic conditions, in order to obtain local values of the frictional pressure gradient. All the thermodynamics and transport properties of the chosen fluids are evaluated with the software Refprop 9.1 [9], developed by NIST, while the data reduction has been implemented with a MATLAB [10] code. The post processing of data has been integrated with the uncertainty analysis for both measured and derived parameters. Table 2 provides a summary of the operating parameters uncertainties (expanded uncertainty with a coverage factor equal to 2) for the whole database.

Table 2. Maximum uncertainty of operating parameters.

Parameter	Maximum uncertainty
(Bubble) saturation temperature $T_{sat,(B)}$	± 0.17 °C
Mass flux G	± 1.3%
Vapor quality x	± 0.3
Pressure gradient	± 29.0%

4. Experimental results

4.1. Experimental procedure and operating conditions

Each test of the experimental campaign for the employed fluids was performed in adiabatic and steady state conditions by setting mass flux, (bubble) saturation temperature and vapor quality values. Particularly, since the new low-GWP mixtures R448A, R452A and R455A have a considerable temperature glide during the evaporation process, the bubble saturation temperature has been fixed by adjusting the thermostatic bath set point. Pure refrigerant R1233zd and new low-GWP mixtures R448A, R452A and R455A have been studied in the same operating conditions such as (bubble) saturation temperature from 25 to 55 °C, mass flux from 150 to 600 kg/m^{2}s in order to compare their performance. Thermodynamic and transfer properties are shown in detail in Table 3 for the chosen fluids at the same bubble saturation temperature of 45 °C (common value for all refrigerants in this experimental campaign). The three mixtures vapor density values are very similar to each other as well as the liquid viscosity ones, whereas R1233zd vapor density value is significantly lower than the others and at the same time its liquid viscosity is substantially higher than the mixtures ones.

Table 3. Thermodynamic and transfer properties for the chosen fluids at the same bubble saturation temperature.

$T_{sat} = 45\ °C$	p_{red}	$\rho_V\ [kg/m^3]$	$\rho_L [kg/m^3]$	ρ_V/ρ_L	$\mu_V\ [\mu Pa-s]$	$\mu_L\ [\mu Pa-s]$	μ_V/μ_L
R1233zd	0.07	13.6	1212	0.01	11.8	364.2	0.03
R448A	0.45	82.6	1003	0.08	13.8	108.6	0.12
R452A	0.53	109.4	1020	0.1	14.4	103.7	0.14
R455A	0.45	68.9	965	0.07	13.2	106.2	0.12

4.2. Effect of the operating parameters on the frictional pressure gradient

Figures 2-5 show the frictional pressure gradient as a function of increasing vapor quality for pure refrigerant R1233zd and R448A, R452A, R455A mixtures, respectively. The effect of operating conditions in terms of mass flux and (bubble) saturation temperature is illustrated. In all cases the pressure gradient firstly increases with the increasing vapor quality until a peak value is reached and then it decreases. As regards the pure refrigerant R1233zd, Figure 2a shows the effect of the mass flux value from 150 to 500 kg/m^{2}s at a saturation temperature of 64.9 °C: due to the increasing flow velocity, the pressure gradient significantly increases with the mass flux. Figure 2b shows the effect of the saturation temperature from 25 to 65 °C at a mass flux value of 304 kg/m^{2}s: the pressure gradient decreases with the increase of the saturation temperature, due to an increased vapor-to-liquid density ratio. This phenomenon is more evident for high vapor qualities, in which the differences between the liquid and vapor velocities are more substantial. By fixing the vapor quality of 0.7, it passes from 20.0 kPa/m at a T_{sat} of 25 °C to 13.4 kPa/m at T_{sat} of 45 °C (-33%) and to 8.4 kPa/m at T_{sat} of 65°C (-58%). For low vapor qualities, instead, all values blend one another and small differenced fall within the uncertainty values.

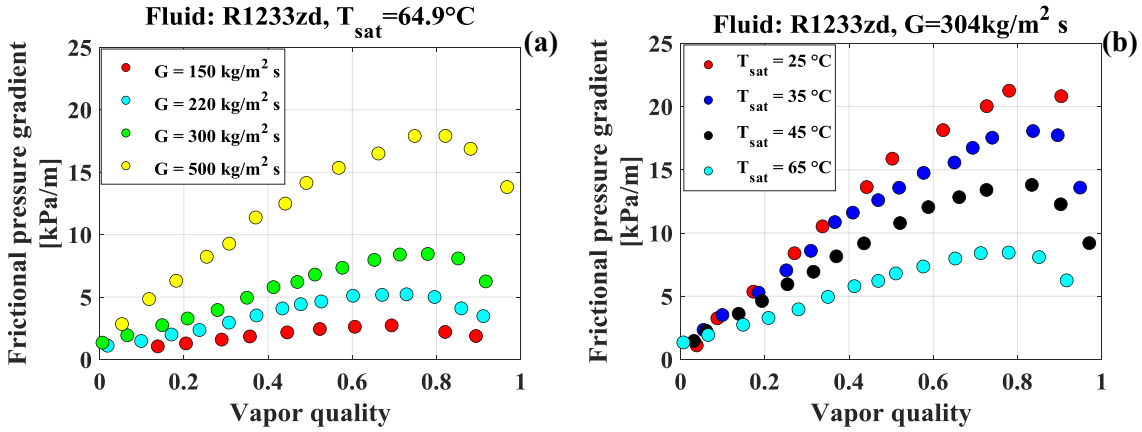

Figure 2. Frictional pressure gradient as a function of vapor quality for R1233zd. Effect of operating parameters. (a) Effect of mass flux for a saturation temperature of 64.9 °C; (b) Effect of the saturation temperature for a fixed mass flux value of 304 kg/m^{2}s.

The same trend in terms of pressure gradient can be observed for the three employed mixtures: as regards the refrigerant R448A, Figure 3a shows the effect of the mass flux value from 150 to 600 kg/m^{2}s at a bubble saturation temperature of 25 °C: the pressure gradient increases with increasing mass flux and it raises from 1.0 kPa/m at a mass flux of 150 kg/m^{2}s to 3.95 kPa/m at 400 kg/m^{2}s (+295%) and to 6.97 kPa/m at 600 kg/m^{2}s (+597%), when the vapor quality is fixed to 0.3. Figure 3b shows the effect of the bubble saturation temperature from 25 to 55 °C at a fixed mass flux of 404 kg/m^{2}s. At a vapor quality of 0.5, the pressure gradient decreases from 6.1 kPa/m at $T_{sat,B}$ of 25°C to 5.0 kPa/m at $T_{sat,B}$ of 35 °C (-18%) and to 1.9 kPa/m at $T_{sat,B}$ of 55 °C (-69%).

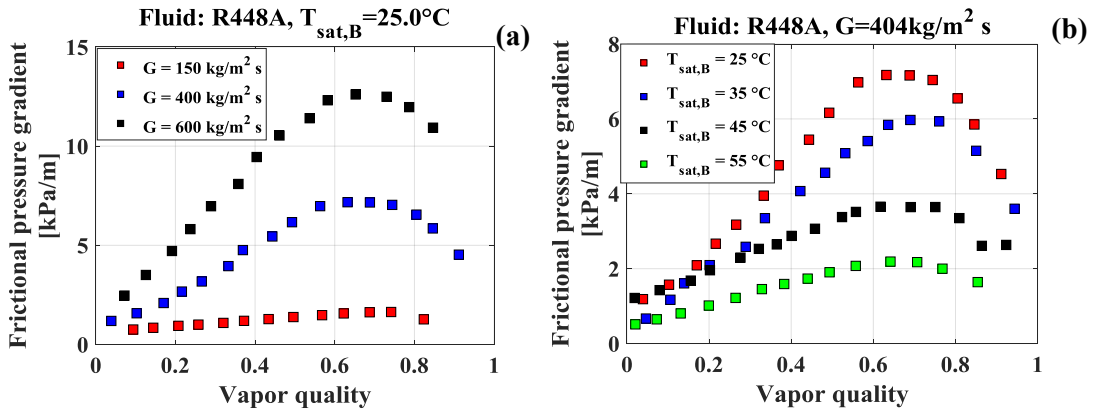

Figure 3. Frictional pressure gradient as a function of vapor quality for R448A. Effect of operating parameters. (a) Effect of mass flux for a bubble saturation temperature of 25.0 °C; (b) Effect of the bubble saturation temperature for a fixed mass flux value of 404 kg/m^{2}s.

For the R452A mixture, three experimental tests were carried-out at the same bubble saturation temperature at a mass flux of 150, 400 and 600 kg/m^{2}s respectively. Figure 4a shows the effect of the mass flux value on the pressure gradient: the pressure gradient increases with the mass flux and it passes from 0.9 kPa/m at a mass flux of 150 kg/m^{2}s 5.7 kPa/m at 600 kg/m^{2}s (+533%) when the vapor quality is set to 0.3. Figure 4b shows the effect of the bubble saturation temperature from 25 to 45 °C at a mass flux value of 402 kg/m^{2}s: the pressure gradient decreases with the increasing bubble saturation temperature. By fixing the vapor quality to 0.7, it reduces from 5.5 kPa/m at $T_{sat,B}$ of 25 °C to 2.6 kPa/m at $T_{sat,B}$ of 45 °C (-111%).

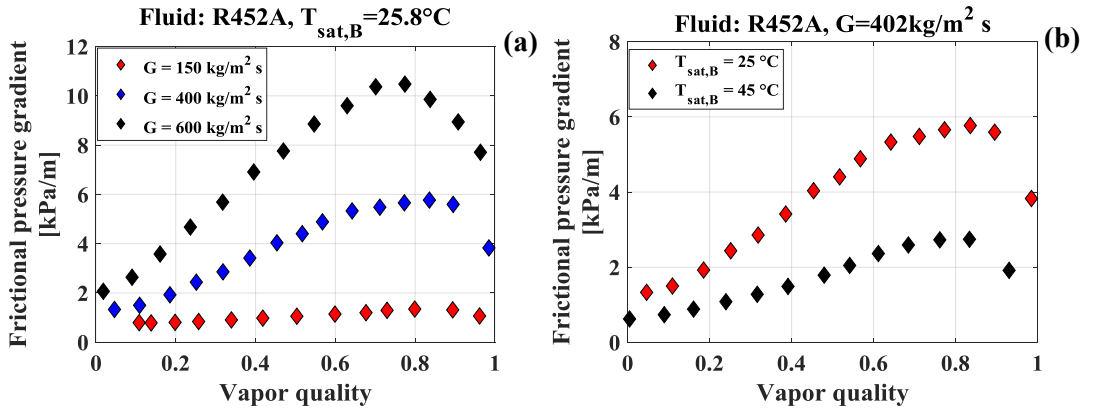

Figure 4. Frictional pressure gradient as a function of vapor quality for R452A. Effect of operating parameters. (a) Effect of mass flux for a bubble saturation temperature of 25.8 °C; (b) Effect of the bubble saturation temperature for a fixed mass flux value of 402 kg/m^{2}s.

Finally, for R455A mixture Figure 5a shows the mass flux effect on the frictional pressure gradient from 300 to 500 kg/m^{2}s at a bubble saturation temperature of 35 °C. Particularly, the frictional pressure gradient grows from 3.3 kPa/m at a mass flux of 150 kg/m^{2}s to 7.6 kPa/m at 500 kg/m^{2}s (+130%) when vapor quality is 0.6. Figure 5b shows the effect of the bubble saturation temperature from 35 to 55 °C at a mass flux value of 495 kg/m^{2}s: the frictional pressure gradient decreases with the bubble saturation temperature. At a vapor quality of 0.5, indeed, it decreases from 6.8 kPa/m at $T_{sat,B}$ of 35 °C to 5.3 kPa/m at $T_{sat,B}$ of 45 °C (-22%) and to 3.9 kPa/m at $T_{sat,B}$ of 55 °C (-42%).

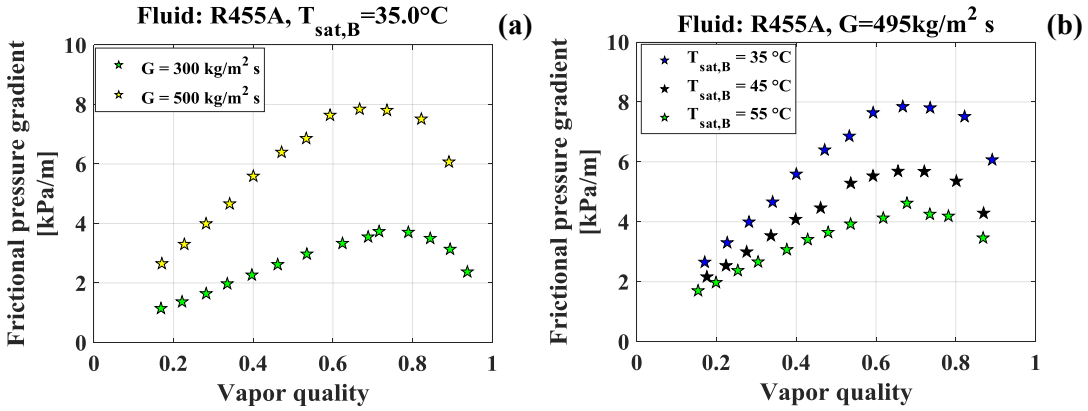

Figure 5. Frictional pressure gradient as a function of vapor quality for R455A. Effect of operating parameters. (a) Effect of mass flux for a bubble saturation temperature of 35.0 °C; (b) Effect of the bubble saturation temperature for a fixed mass flux value of 495 kg/m^{2}s.

4.3. Effect of the working fluid

The frictional pressure gradient of the chosen fluids is shown in Figure 6 for the same bubble saturation temperature of 25 °C and mass flux value of 152 kg/m^{2}s. It is worth noting that, in these conditions, the frictional pressure gradient for pure refrigerant R1233zd is significantly higher than mixtures ones. This behavior can be explained since the low reduced pressure value of R1233zd leads to a low vapor-to-liquid density ratio and consequently a considerable shear stress. As a result, the frictional pressure gradient of R1233zd is more than 100% higher than that of R448A, R452A and R455A. Specifically, when the vapor quality is fixed to 0.3 the frictional pressure gradient value of pure refrigerant R1233zd is 2.9 kPa/m whereas the ones for R448A, R452A and R455A are 1.0 kPa/m, 0.9 kPa/m and 0.85 kPa/m respectively. By fixing the vapor quality value to 0.7 the frictional pressure gradient of R1233zd is 6.6 kPa/m while the ones for R448A, R452A and R455A are 1.6 kPa/m, 1.3 kPa/m and 0.7 kPa/m respectively.

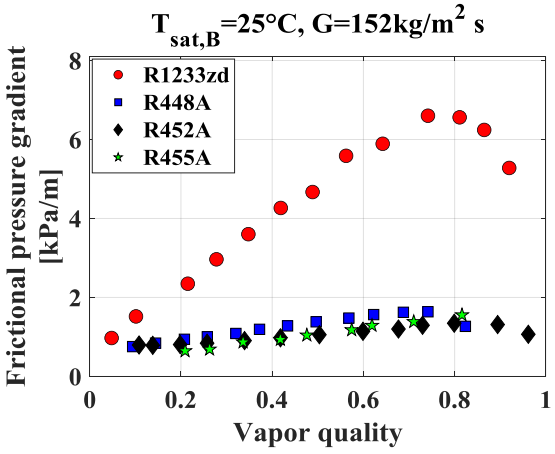

Figure 6. Frictional pressure gradient as a function of vapor quality. Effect of the chosen fluids for a bubble saturation temperature of 25 °C and a mass flux value of 152 kg/m^{2}s.

5. Assessment of the existing prediction methods

More than 10 two-phase pressure drop prediction methods have been implemented, including both homogeneous and drift flux approaches. In this assessment, only the four correlations providing the best statistics (MAPE lower than 40%) are presented, regardless their rationale or the original operating conditions for which they have been developed. Müller-Steinhagen and Heck (1986) [11]

method evaluates the pressure drop as a geometrical average on vapor quality of the all-liquid and all-vapor frictional pressure drop. This method produces a slight underestimation for the refrigerants R1233zd, R448A and R452A, whereas it slightly overestimates the R455A database, with more of 52% of the whole data points falling into a range of error of ±30%. Cioncolini-Thome (2017) [12] and Friedel (1979) [13] correlations consider a separated flow approach of the two-phases for the prediction of the frictional pressure drop: it is found that these methods provide a very good agreement with the whole dataset, with more of 70% and 73% of data points falling into a range of error of ±30% respectively. It is worth noting that the Cioncolini-Thome [12] correlation was originally developed only for annular flow: for this reason, the assessment is carried-out by excluding points that are likely (a visualization section is not available) to fall into the bubbly flow region and in the stratified region. Practically, Figure 7b includes only experiments with vapor qualities higher than 0.3 and at the same time mass flux values higher than 150 kg/m^{2}s. The statistics of this annular flow correlation slightly worsens when applied to the whole dataset, with a MAPE of approximately 30% for all the investigated substances. Finally, Cicchitti et al (1960) [14] method was developed for homogenous flow and displays a slightly underestimation for refrigerants R1233zd, R448A and R452A whereas it provides a very good agreement for the R455A dataset.

Figures 7a-d show the assessment results for the abovementioned correlations and a summary of the statistical parameters (MRPE, MAPE, STD and percentage of data falling into an error range of ±30%, defined as $\delta_{\pm 30\%}$) is provided in Table 4.

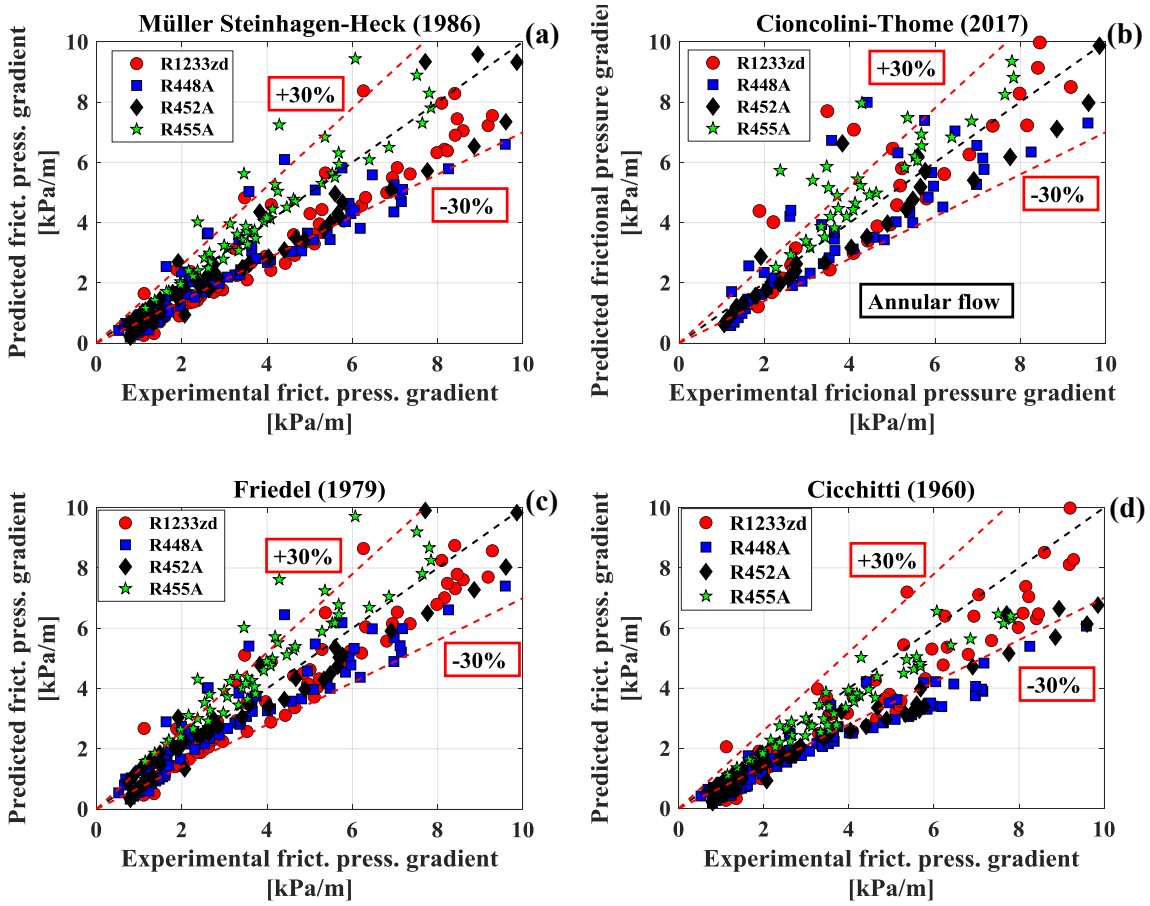

Figure 7. Experimental vs predicted frictional pressure drop. (a) Müller-Steinhagen and Heck (1986) method; (b) Cioncolini-Thome (2017) correlation; (c) Friedel (1979) method; (d) Cicchitti (1960) correlation.

Table 4. Assessment results for the chosen frictional pressure drop predictive methods.

	R1233zd [%]	**R448A [%]**	**R452A [%]**	**R455A [%]**
Müller-Steinhagen and Heck (1986) [11]	MAPE: 25.0 MRPE: -16.6 STD: 24.4 $\delta_{+30\%}$: 65.6	MAPE: 28.8 MRPE: -23.5 STD: 23.2 $\delta_{+30\%}$: 53.9	MAPE: 26.6 MRPE: -23.7 STD: 21.2 $\delta_{+30\%}$: 65.4	MAPE: 11.0 MRPE: 8.9 STD: 18.1 $\delta_{+30\%}$: 92.2
Cioncolini-Thome (2017) [12]	MAPE: 25.2 MRPE: 14.8 STD: 36.4 $\delta_{+30\%}$: 75.8	MAPE: 24.5 MRPE: -6.2 STD: 29.9 $\delta_{+30\%}$: 81.8	MAPE: 18.7 MRPE: -6.9 STD: 22.6 $\delta_{+30\%}$: 81.2	MAPE: 26.4 MRE: 26.4 STD: 29.3 $\delta_{+30\%}$: 71.4
Friedel (1979) [13]	MAPE: 17.8 MRPE: -6.0 STD: 24.3 $\delta_{+30\%}$: 90.6	MAPE: 21.4 MRPE: -7.0 STD: 25.2 $\delta_{+30\%}$: 78.6	MAPE: 18.7 MRPE: -7.6 STD: 22.2 $\delta_{+30\%}$: 80	MAPE: 23.1 MRPE: 13.4 STD: 29.0 $\delta_{+30\%}$: 73.4
Cicchitti et al (1960) [14]	MAPE: 21.3 MRPE: -15.1 STD: 21.9 $\delta_{+30\%}$: 72.9	MAPE: 35.3 MRPE: -35.1 STD: 15.1 $\delta_{+30\%}$: 33.7	MAPE: 35.1 MRPE: -35.1 STD: 15.3 $\delta_{+30\%}$: 29.1	MAPE: 12.0 MRPE: -9.0 STD: 10.4 $\delta_{+30\%}$: 100

6. Conclusions

Experimental adiabatic frictional pressure gradient data of pure refrigerant R1233zd and new low-GWP mixtures R448A, R452A and R455A have been obtained in a 6.00 mm horizontal stainless-steel tube. The main outcomes of this work are summarized as follow:

- The frictional pressure gradient increases with vapor quality up to a peak value before dropping. As regards the effect of the other parameters, it increases with the mass velocity whereas it decreases with the rise of the bubble saturation temperature. This trend has been observed for any operating condition investigated and for any fluid.
- When compared to the three mixtures data, pure refrigerant R1233zd frictional pressure gradients are significantly higher due to its lower reduced pressure and therefore low vapor-to-liquid density ratio: at a mass flux value of 150 kg/m^{2}s and a bubble saturation temperature of 25 °C the percentage difference reaches 560%.
- The assessment of the two-phase frictional pressure gradient predictive methods has shown that the correlation of Friedel [13] provides the best agreement with the experimental data, with more of 73% of data falling into an error band of ±30% MAPE index respectively equal to: 23.1% (R455A), 18.7% (R452A), 21.4% (R448A) and 17.8% (R1233zd).

References

[1] The European Parliament and the Council of the European Union 2014 *Off. J. Eur. Union* **150** 195-230
[2] Huang H, Borhani N, Thome J R 2016 *Int. J. Heat Mass Transfer* **98** 596-610
[3] Xiao J, Hrnjak P 2018 *Int. J. Heat Mass Transfer* **122** 442-450
[4] Zhang J, Kaern M R, Ommen T, Elmegaard B, Haglind F 2019 *Int. J. Heat Mass Transfer* **128** 136-149
[5] Jacob T A, Matty E P, Fronk B M 2020 *Int. J. Refrigeration* **116** 9-22
[6] Mauro A W, Napoli G, Pelella F, Viscito L 2020 *Int. J. Refrigeration* **119** 195-205
[7] Mastrullo R, Mauro A W, Revellin R, Viscito L 2018 *Appl. Therm. Eng.* **145** 251-263
[8] Lillo G, Mastrullo R, Mauro A W, Pelella F., Viscito L 2019 *Appl. Therm. Eng.* **161** 114146
[9] Lemmon E W Mc Linden M O, Huber M L, 2009 *REFPROP NIST* Database **23**
[10] MATLAB 2019a Release, *Mathworks*
[11] Müller-Steinhagen H, Heck K 1986 *Chem. Eng. Process* **20** 297-308
[12] Cioncolini A, Thome J R 2017 *Int. J Multiphase Flow* **89** 321-330
[13] Friedel L1979 *Proceedings*
[14] Cicchitti A, Lombardi C, Silvestri M, Soldaini G, Zavalluilli R 1960 *Energia Nucl.* **7** 407-425